TDHF CALCULATION OF NUCLEAR MOLECULES FROM C12 + C12 TO U238 + U238

R. Y. Cusson[+], H. Stöcker,
G. S. I. Darmstadt, W. Germany

M. R. Strayer, S. Umar, D. A. Bromley
Yale University, New Haven, Conn., U. S. A.

J. A. Maruhn, and W. Greiner
Institut für Theoretische Physik der Universität Frankfurt
D-6000 Frankfurt am Main, West Germany

Abstract

A review of recent applications of the TDHF method to the problem of determining the dynamics of nuclear molecules is made. Two types of nuclear molecular motion are considered; diatomic and polyatomic. Polyatomic motion involes alpha clusters and diatomic motion is defined by requiring a long-lived well defined neck. Some interpretation of the available data is made along these types of dynamics.

1. *Introduction*

The Time Dependent Hartree Fock(TDHF) method[1-7] has shown itself to be rich in nuclear phenomena and continues to stimulate our understanding of nuclear dynamics, in spite of the various conceptual and practical difficulties involved in its use. The first results which came out of TDHF showed that one could make a reasonable account of the fusion cross-section in light systems and the Wilczynski plots of medium ion reactions. Later, higher energy calculations showed that incomplete fusion and preequilibrium nucleon emission[5] were also predicted by the model. In this paper we discuss the latest findings connected with molecular effects in nuclear dynamics.

We will be interested in two types of nuclear molecules. The first type is a diatomic molecule where the nuclear composite system has a well-defined neck and a total rms radius substantially greater than that of the normal compound nucleus. Such molecular shapes may depend on angular momentum and their lifetime could vary greatly as a function of the total J. It is also to be expected that potential pockets connected with the details of the shell correction and spin-orbit potentials will affect not only their stability, but also the prospects for exciting them in nuclear heavy-ion reactions. The second type will be called a polyatomic molecule because it has so far been predicted to

---

[+]Invited speaker; permanent address, Physics Dept., Duke U., Durham, N. C. 27706, U. S. A.

appear as elaborate motions of several alpha clusters in the composite system. This second type had not been predicted so often as the first type in the past, but in view of the strong role played by alpha-like clusters of 2 protons and 2 neutrons in nuclei(quartets), its occurence is, in the end, not so surprising. Polyatomic motions involving bigger clusters such as whole O16 or Ca40 fragments have been postulated[8] but will not be discussed here.

Three different computer codes were used to obtain the results presented here. They use somewhat different interactions and representations for the wavefunction, so that effects seen in several codes have a smaller chance of being an artifact of a particular force and reppresentation. The first code[2] is a momentum space 3-dimensional code using a simplified Skyrme plus Yukawa and Coulomb interaction. This code represents the nucleons as quartets with an effective charge $e(Z_1 + Z_2)/(A_1 + A_2)$ and is in some sense biased toward alpha clusters. It does the time evolution using an extremely accurate 6-th order predictor-corrector and uses the momentum space oportunity to smooth the wavefunctions by cutting off momentum components $\geq 2.\text{fm}^{-1}$. This can be viewed as a gross approximation to the time smoothing effects[9] of the residual interaction, which is otherwise neglected in this work. The second code used is similar to the first one. However, it operates entirely in coordinate space using a 5-point formula for the second derivative on the coordinate grid, and it propagates the states in time using an exponential expansion and an effective Hamiltonian accurate to second order in time. Perhaps because of the high (spurious?) momenta propagated by this code, the polyatomic motions were the least stable with it. The third code[3] works in a rotating frame with axial symmetry and uses a centrifugal potential based on a rigid clutching model for the moment of inertia. Its chief virtue is to allow the use of the full Skyrme interaction without spin-orbit force, and the separation of neutrons and protons. Both SkyrmeII and SkIII interactions were used for the polyatomic motions with similar results.

The TDHF method can only compute the semiclassical trajectories of the collective moments of the composite system as a function of time. The presence of residual interactions induces collisions which, after $t \geq \sim 3\text{x}10^{-21}$ sec. may produce fluctuations and correlations which affect the mean values of the collective trajectories. These collision terms are not included so that the long time behaviour of our results could be adversely affected. Another source of uncertainties stems from the fact that any trajectory calculation involves a potential surface and a set of mass parameters. It is well known that mass parameters are affected by level crossings. Our TDHF work assumes orbit occupation numbers which are time independent, whereas the collision would dictate that levels coming down should see their occupation increased, and so on. This probably affect the fission and fusion behaviour at long time into the reaction. In many TDHF reactions the incident energy is several hundred Mev above the composite system potential energy surface. Yet the single particle friction can quickly absorb this into the thermal doorway states. These states form a small subset of all the compound states at this high excitation energy. On this subset, it appears that the influence of shell

effects is still substantial. As long as the average single particle excitation energy per nucleon in the thermal doorway state is less than the shell energy (≃ 4-8 MeV), the details of the ground state potential energy surface are felt, so that shell correction effects may still influence the dynamics even though the excitation energy is very high. Our work has incorrect shell correction energies for heavy systems because we do not have a spin-orbit term. Thus we can not expect to reproduce reliably those potential pockets which can trap the molecular states[3] and produce long-lived molecules.

Keeping in mind the above pittfalls we can still pursue our study of nuclear molecules provided we exercise care in stating those conclusions which are most sensitive to the errors of the method. We have selected 5 reaction types where TDHF and experiment help us obtain information about nuclear molecules. These are summarised in Table 1 and include i) polyatomic molecules with alpha clusters, ii) medium weight high J_{tot} and E_{tot} diatomic molecules, iii) barrier top potential trapped molecules, iv) asymmetric molecules, and finally v) the di-Uranium system.

2. *Polyatomic Molecules*

The resonances in C12 + C12 scattering[10] are shown in Fig. 1 and a fit using Iachello's U(4) symmetry model is shown[11]. Apart from the missing odd parity levels the agreement with experiment is remarkable and suggests that one should consider intrinsic radial vibrational motion with a dissociation threshold near 7 MeV. The required Morse potential[12] is illustrated in Fig. 2 together with the more conventional C12-C12 real part of the optical potential[13] for two C12 nuclei in their ground state. In spite of the Morse potential's ability to represent the data so well, Fig. 2 shows some of its unphysical properties. To begin with, it has a minimum value where the top of the Coulomb berrier should be. Then, the potential is still non-Coulomb at separations of order 10.fm. It is difficult to se how two C12 nuclei with radii of order 3fm should have a nuclear interaction at such large separation. Finally, it remains puzzling that the potential should be repulsive and non-absorbtive at small radius.

We have made a sudden approximation constrained static Hartree-Fock calculation of the potential between a spherical C12 and a deformed one. These two states of C12 are illustrated in Fig. 3, which shows the H.F. energy vs deformation[13] in C12, and the ground and 4p-4h excited states shapes. The 4p-4h state, (configuration B) shows 3 alpha-like clusters in line and could provide an attractive nuclear interaction at large separations. The sudden potential[14] between A and B, with the long axis of B pointing toward A, and using the simplified Skyrme interaction[1] is shown in Fig. 4. In contrast with Fig. 2, the minimum now occurs at the correct separation of ~7fm. However, the radial width of the potential is smaller than that of the Morse potential and it is somewhat too deep (the Coulomb term is not shown in Fig. 4). In order to fit the observed $\hbar\omega_{vib}$ with this potential we would need a mass parameter larger than the reduced mass of C12+C12. This is puzzling and so is the fact that one can not really expect a sudden potential to exibit the long-lived resonances shown in Fig. 1. An attempt to resolve

this puzzle was made by initialising the TDHF code with the 9fm configuration of Fig. 4. This, if was expected, would give an indication of the time constant for the relative motion of these 2 clusters.

The TDHF motion which resulted from this is shown in Fig. 5. The top left hand frame is the initial configuration and the later times are shown immediatly below and then to the right. The first obervation is that the repulsive part of the sudden potential of Fig. 4 is absent. We have instead, a successive tunnelling of the 3 alphas across the spherical C12 until the initial configuration is reversed. This motion appears quasiperiodic in the TDHF code with a period of about 2.3×10^{-21}sec. corresponding to a harmonic vibrational excitation energy of $\hbar\omega_{vib} \simeq 1.8$MeV. This may be compared with the coefficient a = 1.44MeV in Fig. 1. This is reasonably close in view of the inevitable anharmonicity of the motion. A schematic representation of the potential energy surface of $C12+C12^{*}(7.6\text{MeV}) \leftrightarrow Mg24^{*}$ is shown in Fig. 6, as a function of the mass octupole fragmentation coordinate Q_3 and the mass quadrupole coordinate Q_2. Apart from the expected Mg24 ground state valley, there should be a deep quasimolecular valley which is narrow in the Q_2 direction and long and symmetric about zero in the Q_3 direction. We have indicated schematically with arrows the various observed decay channels of the states in

Table 1: Summary of Reactions Considered.

Reactions	Energy Range	L values	Feature of Interest
C14+α	<<1MeV/A	0	polyatomic vibrations
C12+C12	above Coul. barr.		large dipole transitions
Ar36+α			suspension of s.p. viscosity
Pb208+α			quasi periodic motion
Sr88+Sr88	2-15MeV/A above barr.	$\sim\frac{1}{2}L_{gr}$	very high L-values
Kr86+Er166			diatomic molecules
Kr86+Pb208	top of Coul. barr.	0	long-lived diatomic res.
			potential pocket trapping
Pb208+Ni58	1-3MeV/A above barr.	$0 \leq L \leq L_{gr}$	symmetric breakup of
		~100h	long-lived diatomic molecule
U238+U238	barr. top(~5.9MeV/A)	0<L<150h	deformed U+U entrance channel
	to 6.5MeV/A		→ fast 3-body breakup of
			diUranium composite(6.4MeV/A)

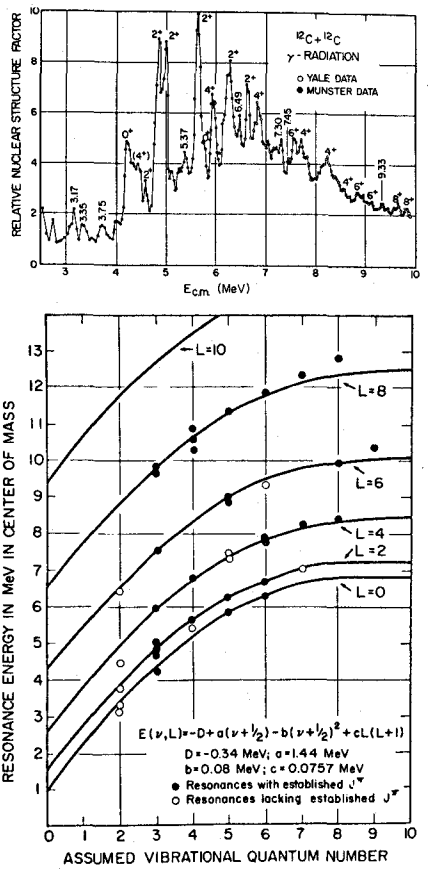

Figure 1. Experimental resonances in C12 + C12 scattering[10].

this valley. Constrained Hartree-Fock calculations of this potential are in progress. It would interesting to also obtain the mass parameter for the octupole motion.

Several types of alpha-cluster motions have been predicted[15] in the light nuclei; this leads us to chose our next example from the reaction C14+α. This reaction is of special interest because the extra 2 neutrons could allow for charge dipole oscillations. A TDHF calculation for this system was performed and showed time-dependent configurations with one alpha-like cluster oscillating across the C14 nucleus. In particular, it was remarkable that this moving cluster did not charge equilibrate while traversing the C14 but retained its 2p-2n character; thus the charge dipole moment shows strong undampened oscillations vs time. These are shown in Fig. 7, where one observes a complex quasiperiodic motion with little damping. The Fourier analysis of this result is in progress; the autocorrelation function and the power spectum should provide additional insight on the nature of the TDHF motion. The time dependent charge quadrupole moment is shown in Fig. 8, the octupole moment is in Fig. 9, and the hexadecaple one is shown in

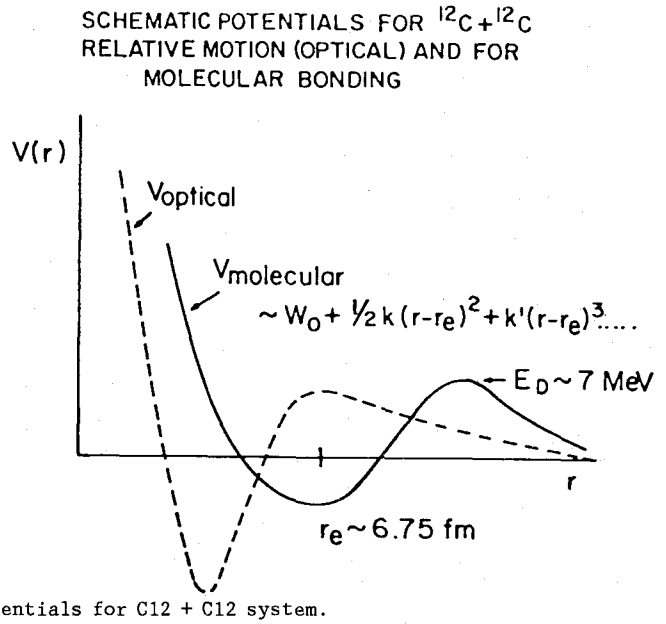

Figure 2. Potentials for C12 + C12 system.

Fig. 10. Whereas the odd multipoles oscillate about zero, the even ones do so about a large average value, so that their % change is much smaller. The crosscorrelation function between the various multipoles is beeing generated and should help determine if the higher multipole oscillations are well correlated with the dipole ones. Neglecting for the moment the energy dependence of the dipole transitions implied by the time dependence, we simply extract the RMS dipole moment from Fig. 7. This is then used to estimate the dipole transition strength inside the 018 rotational band[15] starting at 3.63 MeV(see Fig. 11). This agrees with the experimental values within a factor of 2. We note that there is some odd-even staggering of the energies shown in the inset. This could be

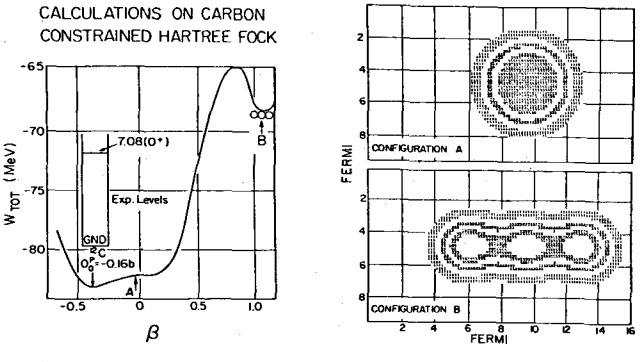

Figure 3. Constrained HF calculations for C12.

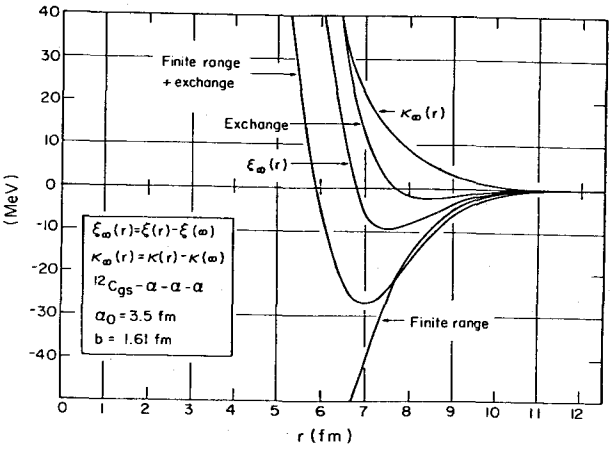

Figure 4. Sudden potential for C12(def.) + C12(gnd).

accounted for by the fact that the even L states are generated by an intrinsic state having no nodes in its vibrational wavefunction, while the odd L one must have one node and one quantum of vibrational excitation. The period observed in the C14+α reaction corresponds to a harmonic excitation energy $\hbar\omega_{vib} \simeq 3$Mev. In a recent[15] U(4) fit of this and the associated rotational band, vibrational energies of this magnitude were required. The moment of inertia implied by the rotational band of Fig. 6 is also consistent with

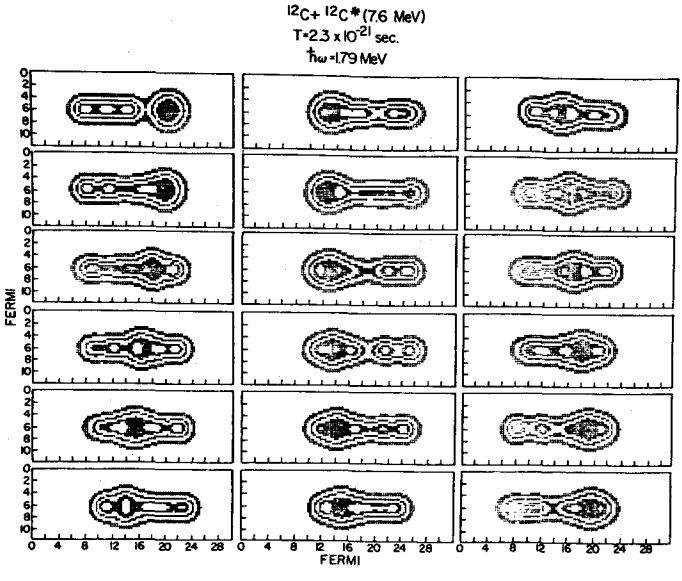

Figure 5. TDHF development of the molecular C12 + C12 system.

the mass quadrupole moment observed in the TDHF calculation. Similarly, the quadrupole transition strengths are consistent with the charge quadrupole moment of Fig. 3.

The motion of alpha-like clusters is also observed with targets of Ar36 and Pb208. Again, no charge equilibration and no damping of the oscillations seem to be taking place. In the case of Ar36, one can clearly see several alpha-like clusters appear in the target during the motion. For a Pb208 target, the transit time of the alpha-like cluster across the nucleus is about 5×10^{-21} sec. Such a picture suggests estimates for the barrier attack frequency in alpha decays. Preliminary calculations[8] imply enhanced and correlated alpha-decay properties for a number of rotational states in Po212.

3. *High Angular Momentum Diatomic Molecules.*

The TDHF method predicts high L-value capture into fast rotating and vibrating composite systems. Figure 12 shows this effect[6] in the reaction[16] Kr86 + Er166 at 12.2 MeV/A. A capture region from $100 \leq L_{in} \leq 270$h is observed. The time dependence of the density is illustrated in Fig. 13 for a non-capture event at $L_{in} = 335$h. The capture events show a similar behaviour at intermediate times: two well-defined clusters, separated by a well-formed neck, rotate about each other. In addition, strong surface waves can usually be seen going around each cluster. The long time behaviour is somewhat uncertain in TDHF, but Fig. 14 illustrates that, even after 5×10^{-21}sec., the system shows no clear indication of a coming separation(for $L_{in} = 215$h). The flux contained in the capture window is not necessary[7] to account for the experimental deep inelastic cross-section. This is illustrated in Fig. 15, where the Wilczynski plots at 6 and 12 MeV are compared with experiment. The motions obtained in the capture region all lie well above the liquid drop limiting values[18] for stable rotations, but the decay mode

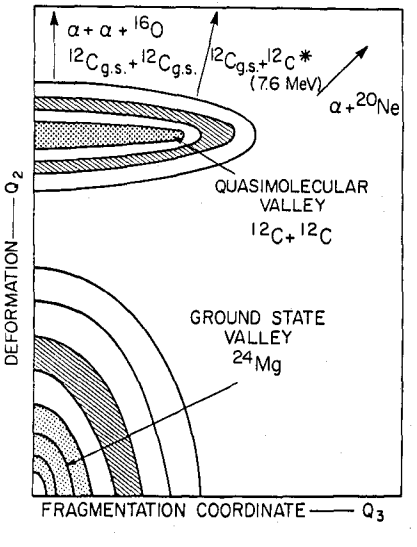

Figure 6. Quasimolecular valley of C12 + C12.

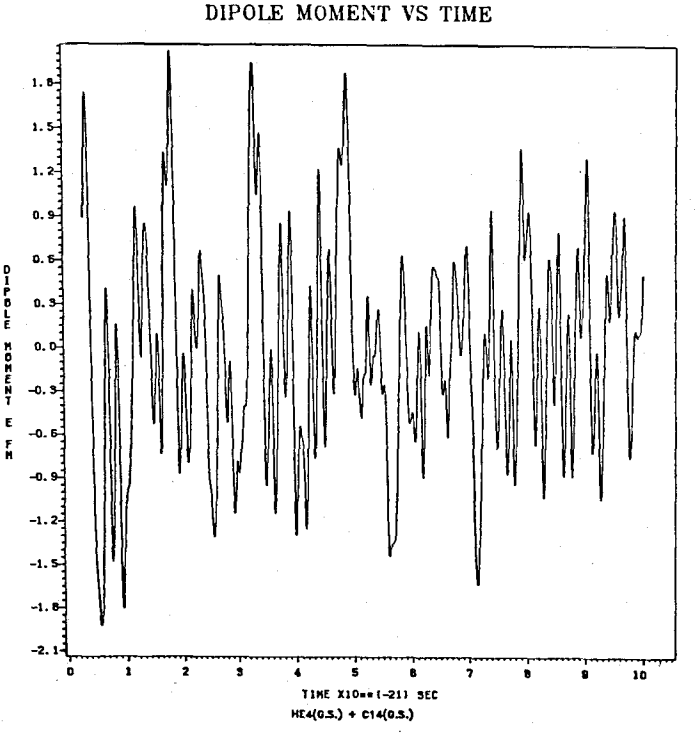

Figure 7. Electric dipole moment of O18 vs time.

need not be two-body, and the lifetime is not known. Although we have observed fast 3-body breakup only once in the U + U system with TDHF, experiments suggest[16,17] that this breakup mode may alrady be be present in the Kr + Er reaction at 12.2 Mev/A. An even stronger suggestion of 3-body breakup is obtained experimentally[17] in the reaction Mo92(14.8MeV/A) + Mo92. Our TDHF calculations for this reaction shows a small capture region. Indeed, a similar calculation of the Sr88 + Sr88 reaction at 20MeV/A also shows a capture region. Of course the TDHF capture process at high L and moderate bombarding energy is subject to substantial fluctuations. They could be due to residual influence of shell effects or to a complicated systematic of hydrodynamic instabilities. So far however, the Mo + Mo 3-body breakup has not been seen in TDHF.

4. *Barrier Top Resonances.*

Heavy ion reactions near the top of the Coulomb barrier and with $L_{in} = 0$ nearly always exibit the phenomenon of sudden neck formation, in TDHF. Depending on the systematic of Coulomb energies, the liquid drop model energy surface for the resulting necked molecular shape can be used to predict the subsequent behaviour of the system. This smooth part of the total energy surface usually predicts fission for heavy systems and fusion for light ones. This picture can be modified by shell effects however. The TDHF shell effects, although incorrect, can thus increase the lifetime of some barrier top

states by a considerable amount. This is illustrated[3] in Fig. 16 for the Kr + La reaction at L = 0. It is believed that there occurs a potential pocket at the fully relaxed energy which traps the system for a long time. A similar effect for Kr + Pb208 has been observed. Such a mechanism could lead to cold fusion in heavy systems, although it is not expected to yield completely stable nuclear molecules.

5. *Symmetric Break up of Nuclear Molecules.*

An interesting class of nuclear molecules shows a stable diatomic necked shape as a result of a balance between the Coulomb force and the centrifugal barrier[6]. This occurs in the Pb + Ni region at 1-3MeV/A above the Coulomb barrier and for $L \leq L_{gr} \sim 100\hbar$. Figure 17 illustrates the possible reaction types under those circumstances. The first horizontal sequence represents ordinary deep inelastic scattering. The second one is fusion-fission where the breakup takes place with a mass drift of some 25 units towards symmetry[19]. The third panel shows actual capture into a long-lived nuclear molecule, while the fourth one shows actual fusion. The different behaviour of these panels are further illustrated in Fig. 18, showing the total RMS radius vs time. All these systems are above the liquid drop limit and should therefore decay. However, the time scale for that is well beyond the capabilities of TDHF even if the calculations could be believed at such long times. Presuming that the dominant decay modes are symmetric

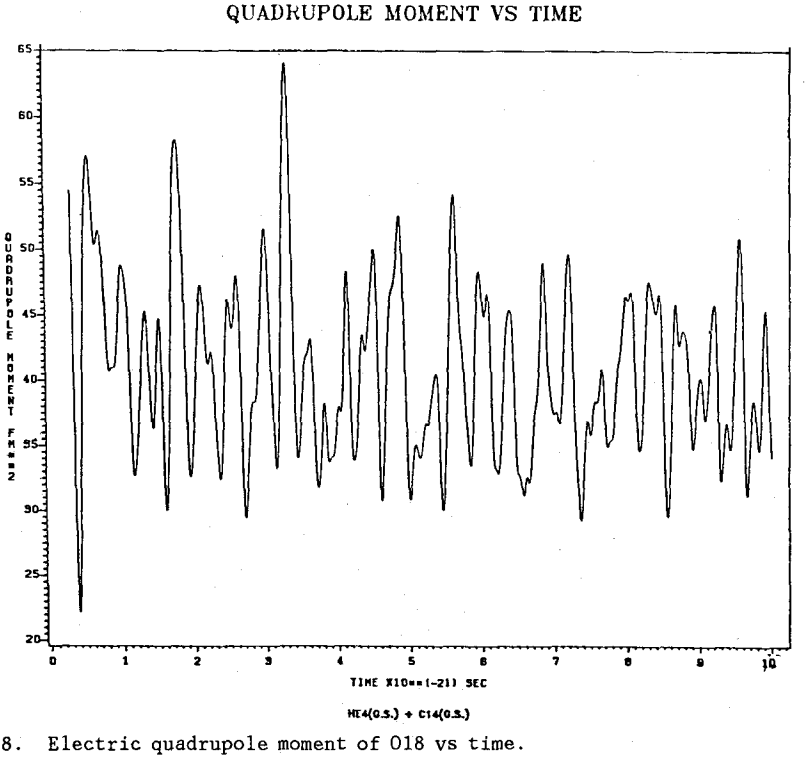

Figure 8. Electric quadrupole moment of O18 vs time.

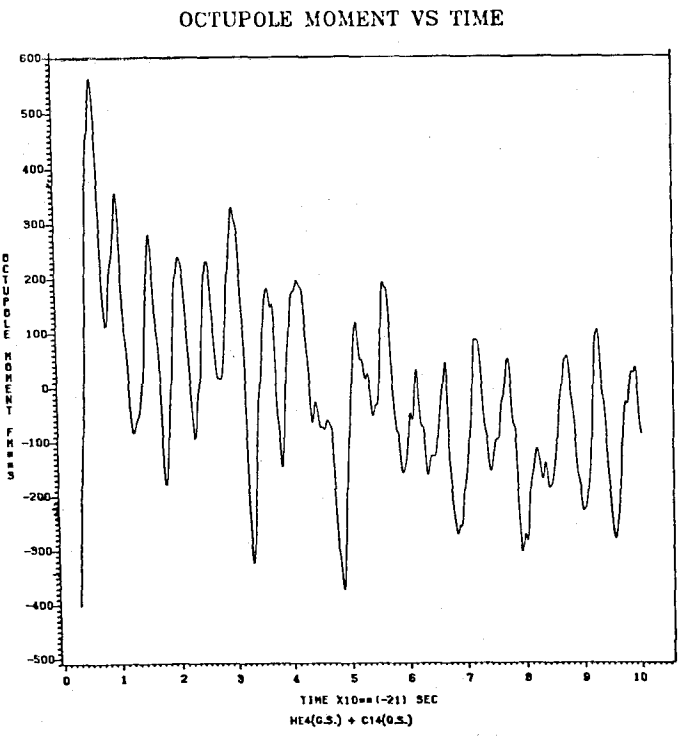

Figure 9. Electric octupole moment of O18 vs time.

fragmentations, we can compare our capture cross- sections with the experimental symmetric fragmentation one. This is done in Fig. 19. The error bars on the computed Pb208 + Ca48 and the U238 + Ca48 cross-sections come from having few impact parameters at each bombarding energy. The dashed line shows the experimental symmetric fragmentation cross-section[19] for Pb208 + Ca48. Here the TDHF result substantially overestimates the cross-section. This appears to be due to a rather unrealistic shell energy for the effective charge quartet model force used for this calculation.

6. *The Di-Uranium Molecule?*

Following recent positron data[20] on the U + U collision, it is interesting to consider again the suggestion[21] of a di-Uranium nuclear molecule. At the barrier top experimental energy of 5.9MeV/A, we have verified that two spherical Uranium nuclei do not even go through a neck formation phase, in TDHF, because of the very large Coulomb repulsion. However, there is a probability that Coulomb excitation can align the deformed Uraniums and even vibrationally excite them into the highly deformed second minimum. Under such circumstances, a neck does form at 5.9MeV/A and it is conceiveable that a fortuitously large amplitude shell correction could lead to a long-lived state of the type seen in Fig. 16. We have looked without success for such a resonance at various initial energies from 5.9 to 6.9 Mev/A, with L=0, at several deformations, using the

axial 2-D code. This of course does not preclude its possible presence if one uses a realistic force with spin-orbit interactions. One novel feature observed in this reaction is the 3-body breakup of the di-Uranium near 6.4MeV/A. The outer fragments each have A ~ 125 and the remaining one has A ~ 226, corresponding to nearly symmetric breakup of each U fragment. These breakups have not so far been detected experimentally for U + U but they have probably been seen for lighter systems such as Kr + Er and Mo + Mo as discussed earlier.

Acknowledgements

We are grateful for the oportunity to utilise the Floating Point Array Processing facilities at the GSI Computation Center where most of the calculations were performed.

References

1. P. Bonche, S. E. Koonin, and J. W. Negele, Phys. Rev. *C13* (1976) 1226.
2. R. Y. Cusson, J. A. Maruhn, and W. A. Meldner, Phys. Rev. *C18* (1978) 2589.
3. K. T. R. Davies,K. R. Sandhia Devi, and M. R. Strayer, Phys. Rev. *C20* (1978) 1372; Phys. Rev. *C24* (1981) 2576.
4. M. Flocard, S. E. Koonin, and M. S. Weiss, Phys. Rev. *C17* (1978) 1682.
5. H. Stöcker, R. Y. Cusson, J. A. Maruhn, and W. Greiner, Phys. Lett. *101B* (1981) 379.
6. H. Stöcker, R. Y. Cusson, H. J. Lustig, A. Gobbi, J. Hahn, J. A. Maruhn, and W. Greiner, Zeitschrift f. Physik *A* (1982) (in press).
7. R. Y. Cusson, J. A. Maruhn, H. Stöcker, Nuclear Physics *A* (1982) (in press).
8. M. Sandalescu (1981) (private communication).
9. R. Balian, and M. Veneroni, Annals of Physics,(N.Y.) *135* (1981) 270.
10. K. A. Erb, and D. A. Bromley, Phys. Rev. *C23* (1981) 2781.
11. F. Iachello, Phys. Rev. *C23* (1981) 2778.
12. K. A. Erb, private communication (1981).
13. R. Y. Cusson, R. Hilko, and D. Kolb, Nucl. Phys. *A270* (1976) 437.
14. P. G. Zint, and U. Mosel, Phys. Lett. *56B* (1975) 563.
15. M. Gai, and D. A. Bromley, (1982), (to be published).
16. A. Olmi, et. al. Phys. Rev. Lett. *44* (1980) 383.
17. A. Gobbi, (1981) (private communication).
18. S. Cohen, F. Plasil, and F. Swiatrcki, Ann. Phys.(N.Y) *82* (1974) 557.
19. A. Olmi et. al., 15th Bormio Winter Meeting on Nuclear Physics, Bormio, Italy (1978) p.724; and to be published.
20. H. Backe, et. al. Phys. Rev. Lett. *40* (1980) 1443.
21. K. Smith, H. Peltz, B. Mueller, and W. Greiner, Phys. Rev. Lett. *32* (1974) 554.

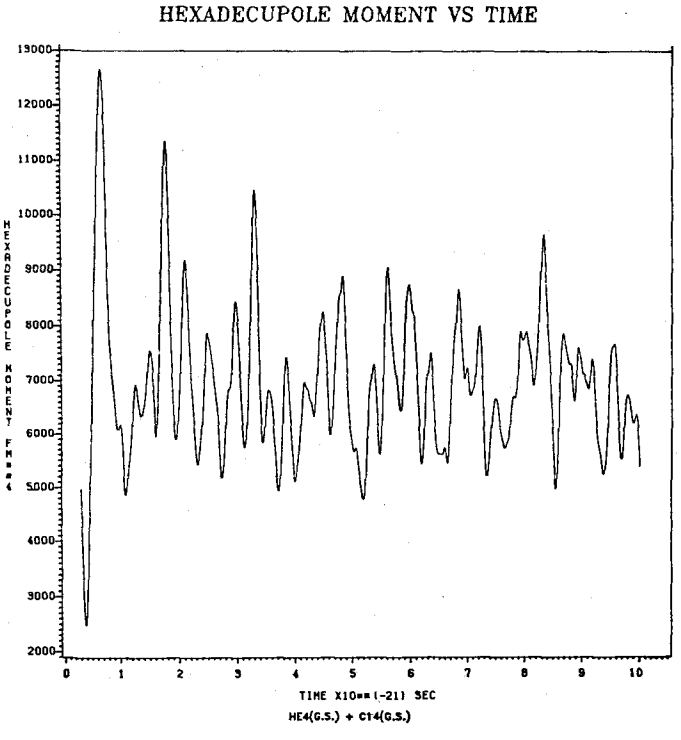

Figure 10. Electric hexadecapole moment of 018 vs time.

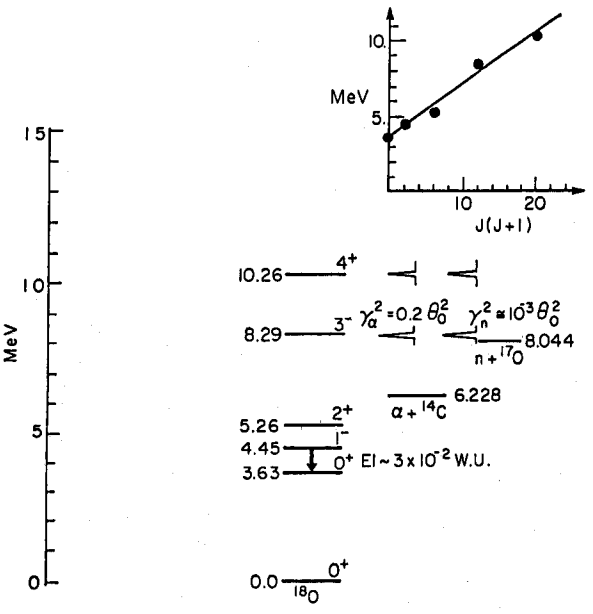

Figure 11. Levels in O18.

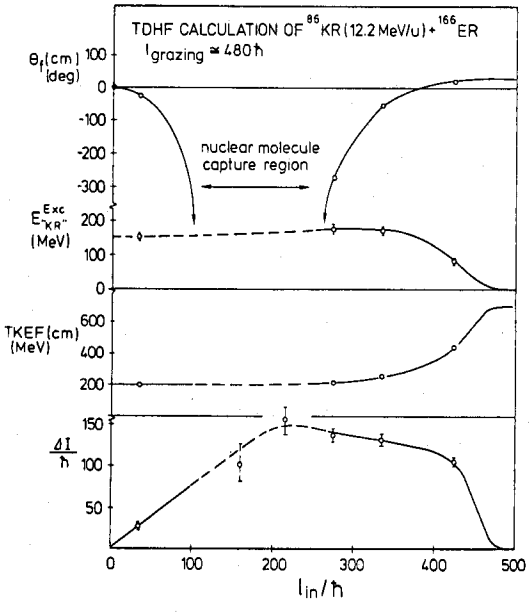

Figure 12. Kr + Er quantities vs L_{in} in TDHF.

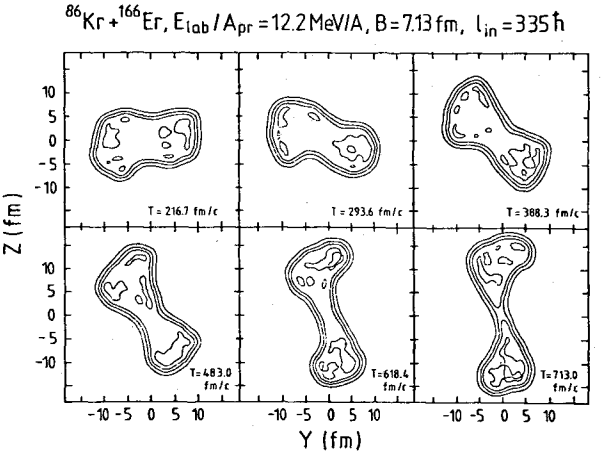

Figure 13. Snapshot of the reaction vs time.

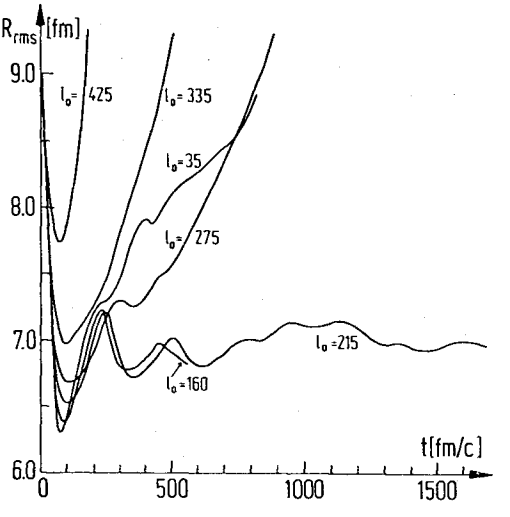

Figure 14. RMS radius of the Kr + Er reaction vs time.

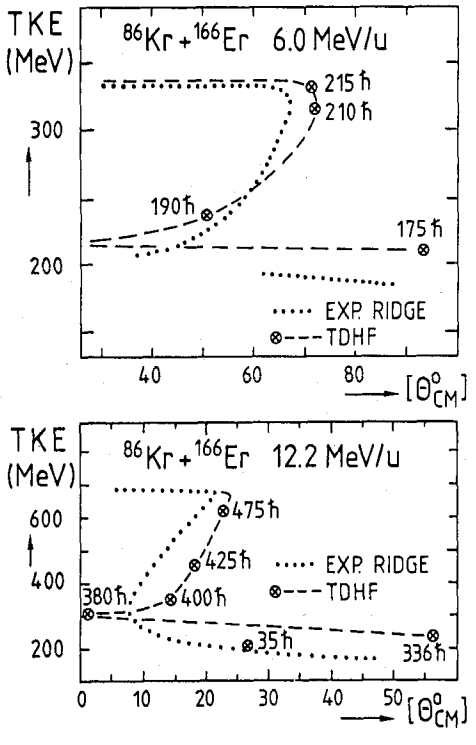

Figure 15. Wilczynski plots ridges compared to experiment[16].

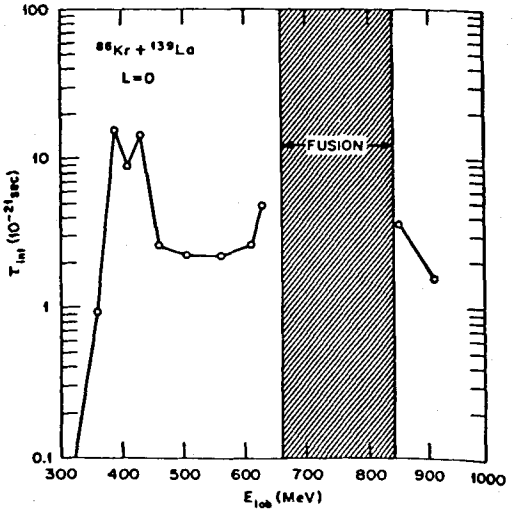

Figure 16. Barrier top resonance in Kr + La.

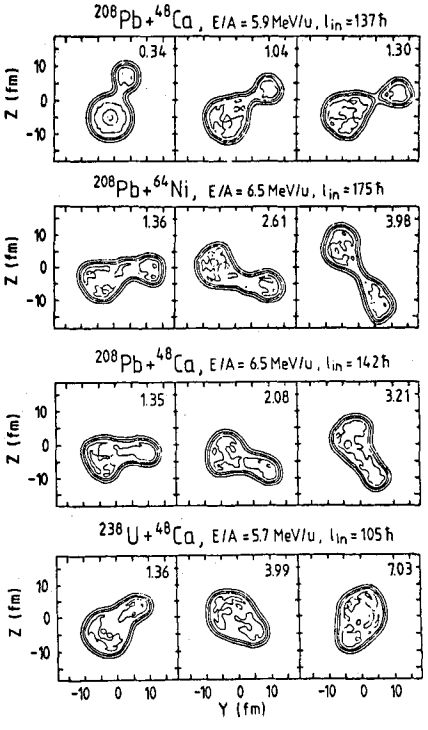

Figure 17. Four types of heavy ion reactions.

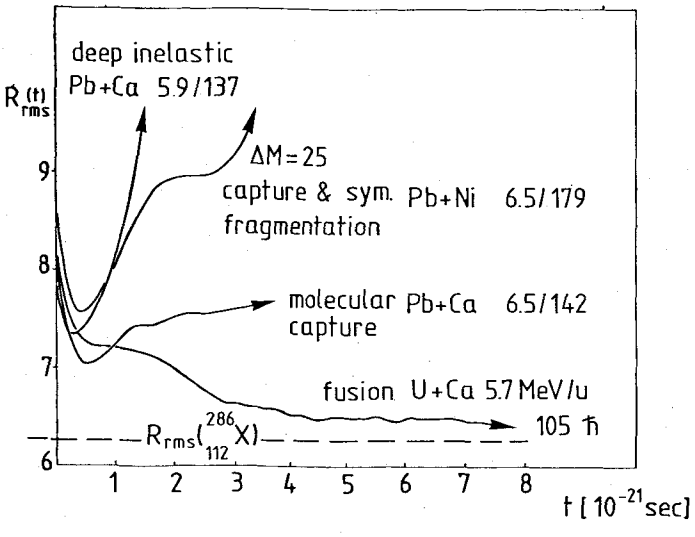

Figure 18. Rms radii vs time.

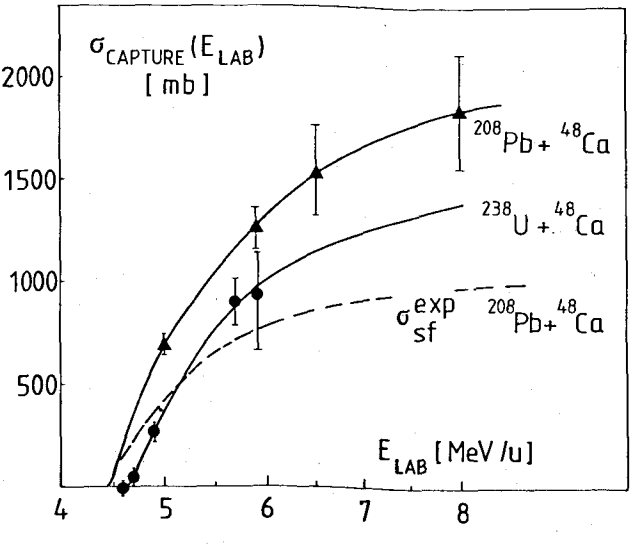

Figure 19. Experimental symm. fragm. cross-section and TDHF values.